



Swansea University  
Prifysgol Abertawe



## Cronfa - Swansea University Open Access Repository

---

This is an author produced version of a paper published in:

*Biosensors and Bioelectronics*

Cronfa URL for this paper:

<http://cronfa.swan.ac.uk/Record/cronfa43849>

---

### **Paper:**

Bollella, P., Sharma, S., Cass, A. & Antiochia, R. (2018). Microneedle-based biosensor for minimally-invasive lactate detection. *Biosensors and Bioelectronics*

<http://dx.doi.org/10.1016/j.bios.2018.08.010>

---

This item is brought to you by Swansea University. Any person downloading material is agreeing to abide by the terms of the repository licence. Copies of full text items may be used or reproduced in any format or medium, without prior permission for personal research or study, educational or non-commercial purposes only. The copyright for any work remains with the original author unless otherwise specified. The full-text must not be sold in any format or medium without the formal permission of the copyright holder.

Permission for multiple reproductions should be obtained from the original author.

Authors are personally responsible for adhering to copyright and publisher restrictions when uploading content to the repository.

<http://www.swansea.ac.uk/library/researchsupport/ris-support/>

## Microneedle-based biosensor for minimally-invasive lactate detection

Paolo Bollella<sup>a</sup>, Sanijv Sharma<sup>b</sup>, Anthony Edward George Cass<sup>c</sup>, Riccarda Antiochia<sup>a,\*</sup>

<sup>a</sup>Department of Chemistry and Drug Technologies - Sapienza University of Rome, Rome, Italy

<sup>b</sup>College of Engineering - Swansea University, Swansea, Wales

<sup>c</sup>Department of Chemistry & Institute of Biomedical Engineering - Imperial College, London, UK

\*Corresponding author.

E-mail address: riccarda.antiochia@uniroma1.it

### Abstract

Here we report the first mediated microneedles-based biosensor for minimally invasive continuous sensing of lactate in the dermal interstitial fluid (ISF). To further demonstrate the capability of microneedle arrays as second generation biosensors we have functionalized gold microneedles with nanocarbons at which mediated electron transfer of lactate oxidase takes place. In particular the gold surface of the microneedles electrode has been modified in 3 subsequent steps: i) electrodeposition of Au-multiwalled carbon nanotubes (MWCNTs); ii) electropolymerization of the mediator, methylene blue (MB); iii) immobilization of the enzyme lactate oxidase (LOX) by drop-casting procedure.

The resulting microneedle-based LOX biosensor displays an interference-free lactate detection without compromising its sensitivity, stability, selectivity and response time.

The performance of the microneedle array, second generation biosensor for lactate detection was assessed in artificial interstitial fluid and in human serum, both spiked with lactate. The results reveal that the new microneedles lactate sensor holds interesting promise for the development of a real-time monitoring device to be used in sport medicine and clinical care.

**Keywords:** Microneedles; Lactate; Minimally invasive sensors; Continuous monitoring; Interstitial fluid

## 1. Introduction

The real-time monitoring of lactate has attracted great interest in the last few years because it is a key analytical target in sport medicine and clinical care (Rassaei et al. 2014). It is known that lactate is an important metabolite formed during the anaerobic metabolism of glucose in muscles. Monitoring of lactate is used to evaluate the maximum performance of an athlete during intensive exercise and endurance-based activities. Lactate concentrations in the blood of healthy individuals ranges from 0.5 to 2 mM at rest rising to 15 mM during exercise and 25mM under intense physical exercise (Brooks 1985; Goodwin et al. 2007; Phypers and Pierce 2006; Stanley et al. 1985). Lactate levels increase also in several pathological conditions, such as cardiac diseases (Karlsson et al. 1975; Valenza et al. 2005) endotoxic shock (Sayeed and Murthy 1981), pulmonary embolism (De Backer et al. 1997), liver disease (Kruse et al. 1987), diabetes and other disorders (Bellomo 2002; Rimachi et al. 2012). Lactate has been recently found to be the major cause of acidification in the microenvironment of cancer cells and therefore plays a key role also in cancer diagnosis (Hirschhaeuser et al. 2011).

Blood lactate levels are therefore currently used as an indicator of both fitness and clinical status. There is a great interest in the development of highly sensitive lactate sensors for general clinical diagnostics, intensive care and sport medicine.

Several classical analytical methods have been used, such as amperometry (Nikolaus and Strehlitz 2008), potentiometry (Shinbo et al. 1979), chemiluminescence (Wu et al. 2005), high-performance liquid chromatography (Omole et al. 1999) and magnetic resonance spectroscopy (Ren et al. 2013). However, these methods have known drawbacks, as they are often time-consuming, expensive and require laboratory equipment and trained personnel.

Amperometric biosensors represent valid alternatives as they allow accurate and cost-effective determination of lactate in real time with improved sensitivity and selectivity.

Numerous amperometric lactate biosensors based on both lactate oxidase (LOX) and lactate dehydrogenase (LDH) immobilized with different strategies on different electrochemical platforms have been previously reported (Agüí et al. 2009; Avramescu et al. 2001; Chen et al. 2017; Collier et al. 1998; Ghamouss et al. 2006; Hickey et al. 2016; Hong et al. 2002; Lamas-Ardisana et al. 2014; Piano et al. 2010; Rathee et al. 2016; Shimomura et al. 2012). Most of them use blood as the matrix for the analytical detection of lactate with the obvious drawback of having to do repeated finger pricks with the consequent discomfort. Researchers have been recently exhorting the use of minimally invasive sensors to measure lactate concentrations in different biological fluids, such as sweat (Abrar et al. 2016; Anastasova et al. 2017; Jia et al. 2013), saliva (Kim et al. 2014; Petropoulos et al. 2016) and tears (Thomas et al. 2012). Unfortunately, these sensors cannot be as

accurate as blood tests because the content of sweat, saliva and tears is more variable as it is can be influenced by other parameters such as the presence of microbes on the skin (in the case of sweat and tears) or by food ingestion (in the case of saliva). The rate of sweating is moreover highly dependent on exercise, temperature and where on the body the measurements are made. Additionally, people aren't always sweating or crying. In many applications outside athletics it is necessary to use wearable bands to locally stimulate sweating.

Microneedle array based biosensors represent an interesting approach as they measure lactate in an under-exploited physiological matrix, the dermal interstitial fluid (ISF), the fluid that bathes the viable tissue of skin. The interstitial fluid is definitely a more accessible and more reproducible matrix and it seems to be a most suitable human body fluid for the minimally invasive detection of lactate. The ISF microenvironment offer a minimally invasive skin compartment in which to measure biomarkers, many of which show a good correlation with venous blood (Paliwal et al. 2013; Sharma et al. 2017). Due to the small dimensions of the microneedles (1 mm length), they can penetrate the stratum corneum but they do not reach deep into the sub-cutaneous tissue, unlike the needle sensors used, for example, in commercially available continuous glucose monitoring (CGM) devices. Measurements are made in the upper part of dermal interstitial compartment where no blood vessels and no nerve endings are present (Sharma et al. 2017). For these reasons, compared to other continuous monitoring devices, the microneedle arrays offer the following advantages: i) minimal invasiveness, thanks to their small dimensions; ii) reduced biofouling effects, as they are changed on a daily basis (24-48 hours maximum) while the other devices are implanted for 7-14 days; iii) larger currents because of their larger electrode surface areas. Moreover, the minimally invasive nature of the microneedle arrays suggests that they are associated with less skin irritation, reduced pain and tissue trauma, lower risk of local infection and lower risk of bleeding. A full recovery is observed within 24 hours of removal (El-Laboudi et al. 2013) and often less.

Initial efforts have been focused on using the microneedle arrays based devices for transdermal delivery of drugs and vaccines (El-Laboudi et al. 2013; Windmiller et al. 2011). Recently, the microneedles have been employed for the development of minimally invasive continuous analytical sensors. In this regards, the first studies have applied microneedle arrays for the continuous monitoring of glucose (Miller et al. 2016; Sharma et al. 2016; Valdés-Ramírez et al. 2014). Subsequently, a few studies have described the development of microneedle based biosensors for the detection of lactate (Miller et al. 2012; Sharma et al. 2017), alcohol (Mohan et al. 2017) and beta-lactams (Rawson et al. 2017). However, there are no publication where microneedle arrays have been shown to function as second generation biosensors (Ventrelli et al. 2015). Most of them

are based on the detection of the hydrogen peroxide produced during the LOX catalysed reaction and so detection occurs at a high overpotential where interferences by other electroactive species which may be present in real samples can be problematic (Abrar et al. 2016).

The present work describes the first example of a mediated pain free microneedle-based biosensor for the continuous monitoring of lactate in the ISF. The gold surface of the microneedles has been modified by electrodeposition of Au-multiwalled carbon nanotubes (MWCNTs) and successively by electropolymerization of the redox mediator, methylene blue (MB). Functionalization of the Au-MWCNTs/polyMB platform with the LOX enzyme by drop casting procedure enabled the continuous monitoring of lactate in artificial interstitial fluid and in human serum.

The interesting analytical performances exhibited by the new microneedles based biosensor makes it a promising tool as a minimally invasive wearable monitoring device for continuous monitoring of lactate to be used in sport medicine and clinical care.

## 2. Experimental

### 2.1 Chemicals and reagents

3-(N-morpholino)propanesulfonic acid (MOPS), 4-(2-Hydroxyethyl)piperazine-1-ethanesulfonic acid (HEPES), ammonium chloride (NH<sub>4</sub>Cl), ascorbic acid (AA), boric acid, calcium chloride (CaCl<sub>2</sub>), D-(-)-glucose (Glc), ferricyanide (Fe(CN)<sub>6</sub><sup>3-</sup>), ferrocyanide (Fe(CN)<sub>6</sub><sup>4-</sup>), human serum from human male AB plasma (USA origin, sterile-filtered), magnesium sulfate (MgSO<sub>4</sub>), methylene blue (MB), multi-walled carbon nanotubes (MWCNTs), potassium chloride (KCl), potassium nitrate (KNO<sub>3</sub>), saccharose, sodium acetate (CH<sub>3</sub>COONa), sodium tetraborate, sodium chloride (NaCl), sodium L-lactate, sodium phosphate dibasic (Na<sub>2</sub>HPO<sub>4</sub>), sodium phosphate monobasic (NaH<sub>2</sub>PO<sub>4</sub>), sulfuric acid (H<sub>2</sub>SO<sub>4</sub>), tris(hydroxymethyl)aminomethane (TRIS) and uric acid (UA) were obtained from Sigma Aldrich (St. Louis, MO, USA).

Lactate oxidase (LOX) from *Aerococcus Viridans* (Umena et al. 2006) was obtained from Creative Enzyme Ltd. The LOX (activity 106 U/ml) was dissolved in a phosphate buffer at pH 6.5, divided into aliquots, and kept at -20 °C until immediately before being used.

All solutions were prepared using Milli-Q water (18.2 MΩ cm, Millipore, Bedford, MA, USA).

### 2.2 Electrode preparation and modification

#### 2.2.1 Gold planar electrodes

Polycrystalline gold electrodes (AuE) (d=2 mm, AMEL, Milano, ITALY) were cleaned by incubation in Piranha solution for 2 min (1:3 mixture of conc. H<sub>2</sub>O<sub>2</sub> with H<sub>2</sub>SO<sub>4</sub>, *CAUTION: Piranha solution is especially dangerous, corrosive and may explode if contained in a closed*

vessel, it should be handled with special care), then with polishing cloths with deagglomerated alumina slurry of 1  $\mu\text{m}$  diameter (SIEM, Bologna, ITALY), successively sonicated in ultrapure water for 5 min and finally electrochemically cleaned in 0.5 M  $\text{H}_2\text{SO}_4$  by cycling 20 times between  $-0.3$  and  $1.7$  V vs. SCE at a scan rate of  $300$   $\text{mV s}^{-1}$ . Polycrystalline gold electrodes were modified by electrodeposition of Au-MWCNTs sweeping the potential between  $0.8$  and  $0$  V vs. SCE for 25 scans at  $50$   $\text{mV s}^{-1}$  in a suspension containing  $5$   $\text{mg mL}^{-1}$  of MWCNTs ( $10$  mM  $\text{HAuCl}_4$  in  $2.5$  M  $\text{NH}_4\text{Cl}$ ) (Dai and Compton 2006). The modified electrodes were characterized in  $5$  mM  $\text{Fe}(\text{CN})_6^{3-/4-}$  ( $50$  mM PBS buffer pH  $7.4$  +  $137$  mM  $\text{NaCl}$ ) in order to determine the electroactive surface area, heterogeneous electron transfer rate constant ( $k^0$ ,  $\text{cm s}^{-1}$ ) and roughness factor ( $\rho$ ). Afterwards, the so prepared AuE/Au-MWCNTs were further modified by electrodeposition of pMB sweeping the potential between  $-0.4$  and  $1.2$  vs. SCE in  $0.25$  mM MB solution ( $0.02$  M borate buffer pH  $9.14$ , supporting electrolyte  $0.1$  M  $\text{KNO}_3$ , sweep rate  $50$   $\text{mV s}^{-1}$ ) (Karyakin et al. 1999). Next,  $5$   $\mu\text{L}$  of LOX were drop-cast onto the modified electrode and left to dry at room temperature. Finally, the electrode was gently rinsed with  $50$  mM PBS buffer (pH  $7.4$ ) and stored at  $4^\circ\text{C}$  overnight.

### 2.2.2 Au microneedles electrodes

The microneedle array base structures were fabricated in polycarbonate at Glasgow University, as described in detail previously (Cass and Sharma 2017) and metallised by Torr Scientific Ltd (Bexhill). They consist of a polycarbonate structure ( $1.0 \times 1.0 \times 0.2$  cm) consisting of 64 microneedles perpendicular to the base plate arranged as four  $4 \times 4$  arrays (pyramid dimensions: base  $0.06$  cm, height  $0.1$  cm;  $4 \times 4$  array area:  $0.2$   $\text{cm}^2$ ). Three of them have been metallized with gold and are used as working electrodes and one has been metallized with silver. However in this work, *in vitro*, an external saturated calomel electrode was used as the reference electrode.

The microneedle electrodes were electrochemically cleaned in  $0.5$  M  $\text{H}_2\text{SO}_4$  by cycling 20 times between  $-0.3$  and  $1.7$  V vs. SCE at a scan rate of  $300$   $\text{mV s}^{-1}$  and successively modified by electrodeposition of Au-MWCNTs, characterized in  $5$  mM  $\text{Fe}(\text{CN})_6^{3-/4-}$  in order to determine the electroactive surface area, heterogeneous electron transfer rate constant ( $k^0$ ,  $\text{cm s}^{-1}$ ) and roughness factor ( $\rho$ ) and finally modified by electrodeposition of pMB and by drop casting of LOX, according to the same procedures as reported for the gold planar electrodes (paragraph 2.2.1).

### 2.3 SEM experiments

Scanning electron microscopy (SEM) measurements were performed with High-Resolution Field Emission Scanning Electron Microscopy (HR FESEM, Zeiss Auriga Microscopy, Jena, Germany).

All samples were prepared according to the modification protocol, as reported in section 2.2, using gold plates (25 Å~ 25 Å~ 1 mm, ALS Co. Ltd., Tokyo, Japan) instead of gold electrodes and Au microneedles electrodes.

#### *2.4 Preparation of artificial interstitial fluid*

The artificial interstitial fluid (ISF) was prepared by mixing 2.5 mM CaCl<sub>2</sub>, 5.5 mM glucose, 10mM Hepes, 3.5 mM KCl, 0.7 mM MgSO<sub>4</sub>, 123 mM NaCl, 1.5 mM NaH<sub>2</sub>PO<sub>4</sub>, 7.4 mM saccharose. The pH was adjusted to pH 7.4 (Saito et al. 2017).

#### *2.5 Electrochemical measurements*

Cyclic voltammetry and amperometric experiments were performed by using a PGSAT204N potentiostat (Eco Chemie, The Netherlands) controlled by Nova 2.1 software (Eco Chemie, The Netherlands) with a conventional three-electrodes electrochemical cell equipped with a modified gold planar electrode or Au microneedles as working electrodes, a saturated calomel electrode (SCE, 244 mV vs. NHE, Cat. 303/SCG/12, AMEL, Milano, Italy) and a glassy carbon rod electrode (d = 2 mm, Cat. 6.1241.020, Metrohm, Herisau, Switzerland) were used as reference and counter electrodes, respectively. The temperature-controlled experiments were carried out by using a thermostatic bath (T ± 0.01 °C, LAUDA RM6, Delran, NJ, USA).

### **3. Results and discussion**

#### *3.1 Microneedles surface functionalization*

The working gold surface of the microneedles has been functionalized initially by electrodeposition of Au-multiwalled carbon nanotubes (MWCNTs), followed by electropolymerization of methylene blue (MB) and finally by immobilization of the enzyme lactate oxidase (LOX) by drop-casting procedure (Fig. 1C).

SEM images were used to evaluate the physical appearance and the surface characteristics of the gold microneedles electrode before and after the electrodeposition of Au-MWCNTs, obtained by cycling the potential between 0.8 and 0 V for 25 cycles. Fig. 2 shows the SEM images relative to the bare gold microneedles electrode (Fig. 2A) and to the Au-MWCNTs microneedles electrode at two different magnifications (Fig. 2B and C). The optimal surface coverage obtained is probably due to the initial reduction of Au<sup>3+</sup> to Au<sup>0</sup> with the formation of Au nanoparticles onto the electrode surface which allow the entrapment of the MWCNTs. This process is further facilitated by the formation of stacking interactions between the nanotubes allowing a good coating. The unmodified and the Au-MWCNTs modified microneedles electrodes were successively characterized by cyclic

voltammetry experiments in a solution of  $\text{Fe}(\text{CN})_6^{3-/4-}$  (Fig.1S). It is possible to note the large enhance of the anodic and cathodic peak current densities after the Au-MWCNTs electrodeposition due to the increase of the electroactive surface area. It is interesting to observe that this effect is much more evident in the case of the microneedles electrode (Fig. 1S B) compared to the planar gold electrode (Fig. 1S A), as confirmed by the roughness factor which resulted to be almost ten times higher in the case of the microneedles electrode ( $\rho=301.6 \pm 1.6$ ) compared to the planar electrode ( $\rho=39.5 \pm 0.6$ ). This result can be ascribed to the fact that the particular geometry of the microneedles might allow a better electrodeposition of the MWCNTs and therefore a larger electroactive surface area. The heterogeneous electron transfer rate constants ( $k^0$ ,  $\text{cm s}^{-1}$ ) have also been calculated using the extended method which merges the Klingler-Kochi and Nicholson and Shain methods for totally irreversible and reversible systems (Lavagnini et al. 2004, 2007). The  $k_0$  value obtained in the case of the Au microneedles/Au-MWCNTs electrode resulted to be much higher ( $k_0= 16.3 \pm 0.4 \times 10^3 \text{ cm s}^{-1}$ ) than that obtained in the case of the planar Au electrode modified with Au-MWCNTs ( $k_0 = 2.7 \pm 0.9 \times 10^3 \text{ cm s}^{-1}$ ), showing a faster electron transfer kinetics.

The Au-MWCNTs microneedles electrode was successively modified by electrodeposition of the redox mediator methylene blue, by cycling the potential values from -0.4 to 1.2 V vs. SCE for 25 cycles in borate buffer pH 9.1. Fig. 2D show the SEM image of the Au microneedle/Au-MWCNTs/polyMB modified electrode. The voltammetric profile of the formation of the polymeric film shows two couples of redox peaks (Fig. 2S). As the electropolymerization process takes place, the couple of peaks which appears at more negative potentials decreases and a new set of peaks appears at more positive potentials. This response is typical of a polymer-type redox activity, which is usually shifted to more positive potentials compared to the monomer (Karyakin et al. 1999). The cyclic voltammogram of the Au-MWCNTs/polyMB modified microneedle electrode is shown in Fig. 3S. Two pairs of quasi-reversible redox peaks are clearly visible in the voltammogram. The first one corresponds to the monomer, the additional one to the polyMB and is located at a 200 mV more anodic potential, according to data reported in literature for electropolymerized amines (Braun et al. 2017; Liu and Mu 1999).

### *3.2 Electrochemical characterization of lactate sensor*

Lactate biosensors were prepared by drop-casting LOX enzyme onto the Au-MWCNTs/pMB microneedle electrode surface. In order to optimize the enzyme concentration, different biosensors were prepared by drop-casting different LOX amounts on the microneedles surface. The effect of enzyme loading on the current response was investigated in the range from 1U to 5 U of LOX. The current density increased when the concentration of LOX increased from 1 to 1.5 U showing a



slight decrease at higher enzyme concentrations (Fig. 4S A). The amount of enzyme is therefore rate limiting at low enzyme amounts loaded but at higher concentrations the reaction becomes limited by other factors. A concentration of 1.5 U was chosen for further experiments. The biosensor performance was also tested by varying the concentration of MWCNTs used during the electrodeposition process and the electrodeposition number cycles (Fig. 4S B and C). The results confirmed that the highest current signal was obtained by cycling the potential for 25 cycles in a solution of 5 mg/mL MWCNTs, conditions used for the microneedle surface functionalization experiments.

A comparative cyclic voltammogram of the Au-MWCNTs/pMB/LOX microneedle electrode in the absence and in the presence of lactate is shown in Fig. 3 A. The black curve shows no significant difference with the CV of the modified electrode without enzyme (curve not shown), thus indicating that no significant change has been observed after the immobilization of LOX. It is possible to note a very good electrocatalytic current with an onset potential of -90 mV, close to the redox potential of the mediator pMB ( $E_0 = -95$  mV vs. SCE). Such low potential for lactate oxidation reflects the efficient electron donor-acceptor interactions between the carbon nanotubes and the mediator, which supports the shuttling of the electrons between the redox center of the enzyme and the electrode surface. A potential of +0.15 V vs SCE reference electrode was thus selected for further experiments. If we compare these results with those obtained with a planar gold electrode modified exactly in the same way, we can see that the electrocatalytic current obtained with the microneedles is almost three times higher than that obtained with the planar electrode (Fig. 3 B). This result can be explained by the fact that the geometry of the microneedle electrodes might enable faster diffusion of the substrate to the electrode surface (Belding et al. 2010; Menshykau et al. 2008).

The analytical response of the microneedle biosensor towards lactate was evaluated by chronoamperometry (Fig. 3 C). The calibration curve for lactate detection, shown in Fig. 3 D, indicates a linear range from 10  $\mu$ M to 200  $\mu$ M lactate, a detection limit of 2.4  $\mu$ M (based on  $S/N=3$ ) and a very high sensitivity of 1473  $\mu$ A  $\text{cm}^{-2}$   $\text{mM}^{-1}$  and a correlation coefficient of 0.98 (RSD 5.0%,  $n=3$ ). Additionally, the calibration curve was fitted to the classical Michaelis-Menten kinetic parameters, which resulted in a  $J_{\text{max}}$  of  $733 \pm 19$   $\mu$ A  $\text{cm}^{-2}$  and an apparent Michaelis-Menten constant ( $K_M$ ) of  $0.64 \pm 0.1$  mM.

### 3.3 Effect of pH and temperature on biosensor response

The effects of pH and temperature on the proposed lactate biosensor were evaluated and the results are shown in Fig. 4 A and B. Four different buffers have been tested, acetate, MOPS, phosphate and TRIS buffer in order to cover the range of pHs between 2 and 9. The current signal increased with

pH until a pH value of 7.5, which corresponds to the maximum current signal obtained in both phosphate buffer and TRIS buffer (Fig. 4A). A pH 7.5 in phosphate buffer is therefore chosen for our experiments because phosphate buffer is the closest to physiological conditions. The optimum temperature resulted to be 35 °C, as shown in Fig. 4B. These results are in close agreement with the optimum pH and T values reported in literature for lactate oxidase (Taurino et al. 2016).

#### *3.4 Study of biosensor stability*

The stability and lifetime of the biosensor were investigated by monitoring the signal decrease of the current when the biosensor is used for 20 measurements every day over a period of 30 days for a 0.2 mM lactate solution, as reported in Fig. 4C. The microneedles based biosensor showed a signal decrease of its initial response of less than 10% after 30 days, probably due to a combination of the intrinsic stability of the enzyme, the nanostructuring of the microneedle electrode surface and to the particular geometry of the microneedles themselves.

#### *3.5 Interference study*

The selectivity of the biosensor was studied in order to assess the influence of possible interfering compounds on its response. The signal obtained for a fixed concentration of lactate was compared to that obtained with equal amounts of interfering compounds such as ascorbic acid, uric acid and glucose. No significant currents from interference by these compounds was observed (Fig. 4D). Such high selectivity reflects the low operating potential of the second generation biosensor, due to the combined use of the electropolymerized MB and a nanostructured surface.

#### *3.6 Analysis of artificial interstitial fluid and human serum*

In order to demonstrate the feasibility of the modified microneedles based electrode for the minimally invasive detection of lactate, the biosensor was used to determine the concentration of lactate in artificial interstitial fluid and human blood samples, both spiked with lactate. Fig. 5 shows the calibration plots obtained with artificial ISF and human serum. The response is linear in both case with a similar detection limit, but a narrower linear range compared to that reported previously in phosphate buffer pH 7.5. The sensitivities resulted to be  $800 \pm 38 \mu\text{A cm}^{-2} \text{mM}^{-1}$  in ISF (RSD 4.8%, n=3) and  $180 \pm 9 \mu\text{A cm}^{-2} \text{mM}^{-1}$  (RSD 5.2%, n=3) in human serum, lower than that obtained in phosphate buffer. This result is particularly evident with the measurements carried out in human serum where the measurements may be affected by biofouling effects of the electrode. However, the response obtained in the ISF remains high enough to allow a good detection of lactate

and indicates the potential for the subcutaneous lactate monitoring based on the proposed microneedles based biosensor.

Fig. 6 shows a comparison of the results obtained with other non-invasive amperometric lactate biosensors reported in literature. Lactate was detected in different biological fluids such as sweat, saliva and tears. As we can see, the linear range is broader but the sensitivity obtained is definitely lower than that obtained with the microneedles-based biosensor.

It is important to note that the content of sweat, saliva and tears is more variable compared to the composition of blood and of interstitial fluid. It can be influenced by different factors such as microbes on the skin (in the case of sweat and tears) or by food ingestion (in the case of saliva). Moreover, as people aren't always sweating, in many applications outside athletics it is necessary to use wearable bands to locally stimulate sweating. The interstitial fluid is an accessible and more reproducible matrix and it seems to be the most suitable human body fluid for the minimally invasive measurement of lactose.

#### **4. Conclusions**

This study has demonstrated the design and development of the first example of a second generation minimally invasive biosensor for lactate detection based on microneedle arrays. The new biosensor device is based on the use of a gold microneedles electrode modified with MWCNTs, polymethylene blue and lactate oxidase from *Aereococcus viridans*. The system enables highly sensitive, selective and stable determination of lactate in human interstitial fluid, which suggests that it is a suitable body fluid compared to sweat, saliva and tears, as it is expected to show less variability in its composition. For these reasons the lactate biosensor based on microneedle technology seems to be a promising tool as a wearable device to be used in sport medicine and in clinical care for continuous monitoring of lactate. The biosensor will be further optimized and validated for *in vivo* measurements through clinical studies with healthy volunteers.

Future efforts will focus on integration of the instrumentation for signal processing and wireless communication, as well as on a critical evaluation of the tolerability and biocompatibility of the device.

#### **Acknowledgements**

#### **References**

Abrar, M.A., Dong, Y., Lee, P.K., Kim, W.S., 2016. Bendable electro-chemical lactate sensor printed with silver nano-particles. Scientific reports 6, 30565.

Agüí, L., Eguilaz, M., Peña-Farfal, C., Yáñez-Sedeño, P., Pingarron, J.e.M., 2009. Lactate Dehydrogenase Biosensor Based on an Hybrid Carbon Nanotube-Conducting Polymer Modified Electrode. *Electroanalysis* 21(3-5), 386-391.

Anastasova, S., Crewther, B., Bembnowicz, P., Curto, V., Ip, H.M., Rosa, B., Yang, G.-Z., 2017. A wearable multisensing patch for continuous sweat monitoring. *Biosensors and Bioelectronics* 93, 139-145.

Avramescu, A., Noguier, T., Magearu, V., Marty, J.-L., 2001. Chronoamperometric determination of D-lactate using screen-printed enzyme electrodes. *Analytica chimica acta* 433(1), 81-88.

Belding, S.R., Campbell, F.W., Dickinson, E.J., Compton, R.G., 2010. Nanoparticle-modified electrodes. *Physical Chemistry Chemical Physics* 12(37), 11208-11221.

Bellomo, R., 2002. Bench-to-bedside review: lactate and the kidney. *Critical Care* 6(4), 322.

Braun, W.A., Horn, B.C., Hoehne, L., STÜLP, S., ROSA, M.B., Hilgemann, M., 2017. Poly (methylene blue)-modified electrode for indirect electrochemical sensing of OH radicals and radical scavengers. *Anais da Academia Brasileira de Ciências(AHEAD)*, 0-0.

Brooks, G.A., 1985. Anaerobic threshold: review of the concept and directions for future research. *Medicine and science in sports and exercise* 17(1), 22-34.

Cass, A.E., Sharma, S., 2017. Microneedle enzyme sensor arrays for continuous in vivo monitoring. *Methods in enzymology*, pp. 413-427. Elsevier.

Chen, Q., Sun, T., Song, X., Ran, Q., Yu, C., Yang, J., Feng, H., Yu, L., Wei, D., 2017. Flexible electrochemical biosensors based on graphene nanowalls for the real-time measurement of lactate. *Nanotechnology* 28(31), 315501.

Collier, W., Lovejoy, P., Hart, A., 1998. Estimation of soluble L-lactate in dairy products using screen-printed sensors in a flow injection analyser. *Biosensors and Bioelectronics* 13(2), 219-225.

Dai, X., Compton, R.G., 2006. Direct electrodeposition of gold nanoparticles onto indium tin oxide film coated glass: application to the detection of arsenic (III). *Analytical sciences* 22(4), 567-570.

De Backer, D., Creteur, J., Zhang, H., Norrenberg, M., Vincent, J.-L., 1997. Lactate production by the lungs in acute lung injury. *American journal of respiratory and critical care medicine* 156(4), 1099-1104.

El-Laboudi, A., Oliver, N.S., Cass, A., Johnston, D., 2013. Use of microneedle array devices for continuous glucose monitoring: a review. *Diabetes technology & therapeutics* 15(1), 101-115.

Ghamouss, F., Ledru, S., Ruillé, N., Lantier, F., Boujtita, M., 2006. Bulk-modified modified screen-printing carbon electrodes with both lactate oxidase (LOD) and horseradish peroxidase (HRP) for the determination of L-lactate in flow injection analysis mode. *Analytica chimica acta* 570(2), 158-164.

Goodwin, M.L., Harris, J.E., Hernández, A., Gladden, L.B., 2007. Blood lactate measurements and analysis during exercise: a guide for clinicians. *Journal of diabetes science and technology* 1(4), 558-569.

Hickey, D.P., Reid, R.C., Milton, R.D., Minter, S.D., 2016. A self-powered amperometric lactate biosensor based on lactate oxidase immobilized in dimethylferrocene-modified LPEI. *Biosensors and Bioelectronics* 77, 26-31.

Hirschhaeuser, F., Sattler, U.G., Mueller-Klieser, W., 2011. Lactate: a metabolic key player in cancer. *Cancer research* 71(22), 6921-6925.

Hong, M.-Y., Chang, J.-Y., Yoon, H.C., Kim, H.-S., 2002. Development of a screen-printed amperometric biosensor for the determination of L-lactate dehydrogenase level. *Biosensors and Bioelectronics* 17(1-2), 13-18.

Jia, W., Bandodkar, A.J., Valdés-Ramírez, G., Windmiller, J.R., Yang, Z., Ramírez, J., Chan, G., Wang, J., 2013. Electrochemical tattoo biosensors for real-time noninvasive lactate monitoring in human perspiration. *Analytical chemistry* 85(14), 6553-6560.

Karlsson, J., Willerson, J., Leshin, S., Mullins, C., Mitchell, J., 1975. Clinical Physiology: Skeletal Muscle Metabolites in Patients with Cardiogenic Shock or Severe Congestive Heart Failure. *Scandinavian journal of clinical and laboratory investigation* 35(1), 73-79.

Karyakin, A.A., Karyakina, E.E., Schmidt, H.L., 1999. Electropolymerized azines: a new group of electroactive polymers. *Electroanalysis: An International Journal Devoted to Fundamental and Practical Aspects of Electroanalysis* 11(3), 149-155.

Kim, J., Valdés-Ramírez, G., Bandodkar, A.J., Jia, W., Martínez, A.G., Ramírez, J., Mercier, P., Wang, J., 2014. Non-invasive mouthguard biosensor for continuous salivary monitoring of metabolites. *Analyst* 139(7), 1632-1636.

Kruse, J.A., Zaidi, S.A., Carlson, R.W., 1987. Significance of blood lactate levels in critically III patients with liver disease. *The American journal of medicine* 83(1), 77-82.

Lamas-Ardisana, P.J., Loaiza, O.A., Añorga, L., Jubete, E., Borghei, M., Ruiz, V., Ochoteco, E., Cabañero, G., Grande, H.J., 2014. Disposable amperometric biosensor based on lactate oxidase immobilised on platinum nanoparticle-decorated carbon nanofiber and poly (diallyldimethylammonium chloride) films. *Biosensors and Bioelectronics* 56, 345-351.

Lavagnini, I., Antiochia, R., Magno, F., 2004. An extended method for the practical evaluation of the standard rate constant from cyclic voltammetric data. *Electroanalysis* 16(6), 505-506.

Lavagnini, I., Antiochia, R., Magno, F., 2007. A Calibration-Base Method for the Evaluation of the Detection Limit of an Electrochemical Biosensor. *Electroanalysis* 19(11), 1227-1230.

Liu, J., Mu, S., 1999. The electrochemical polymerization of methylene blue and properties of polymethylene blue. *Synthetic Metals* 107(3), 159-165.

Menshykau, D., Streeter, I., Compton, R.G., 2008. Influence of electrode roughness on cyclic voltammetry. *The Journal of Physical Chemistry C* 112(37), 14428-14438.

Miller, P.R., Narayan, R.J., Polsky, R., 2016. Microneedle-based sensors for medical diagnosis. *Journal of Materials Chemistry B* 4(8), 1379-1383.

Miller, P.R., Skoog, S.A., Edwards, T.L., Lopez, D.M., Wheeler, D.R., Arango, D.C., Xiao, X., Brozik, S.M., Wang, J., Polsky, R., 2012. Multiplexed microneedle-based biosensor array for characterization of metabolic acidosis. *Talanta* 88, 739-742.

Mohan, A.V., Windmiller, J.R., Mishra, R.K., Wang, J., 2017. Continuous minimally-invasive alcohol monitoring using microneedle sensor arrays. *Biosensors and Bioelectronics* 91, 574-579.

Nikolaus, N., Strehlitz, B., 2008. Amperometric lactate biosensors and their application in (sports) medicine, for life quality and wellbeing. *Microchimica Acta* 160(1-2), 15-55.

Omole, O.O., Brocks, D.R., Nappert, G., Naylor, J.M., Zello, G.A., 1999. High-performance liquid chromatographic assay of ( $\pm$ )-lactic acid and its enantiomers in calf serum. *Journal of Chromatography B: Biomedical Sciences and Applications* 727(1-2), 23-29.

Paliwal, S., Hwang, B.H., Tsai, K.Y., Mitragotri, S., 2013. Diagnostic opportunities based on skin biomarkers. *European journal of pharmaceutical sciences* 50(5), 546-556.

Petropoulos, K., Piermarini, S., Bernardini, S., Palleschi, G., Moscone, D., 2016. Development of a disposable biosensor for lactate monitoring in saliva. *Sensors and Actuators B: Chemical* 237, 8-15.

Phypers, B., Pierce, J.M.T., 2006. Lactate physiology in health and disease. *Continuing education in Anaesthesia, critical care & pain* 6(3), 128-132.

Piano, M., Serban, S., Pittson, R., Drago, G., Hart, J.P., 2010. Amperometric lactate biosensor for flow injection analysis based on a screen-printed carbon electrode containing Meldola's Blue-Reinecke salt, coated with lactate dehydrogenase and NAD<sup>+</sup>. *Talanta* 82(1), 34-37.

Rassaei, L., Olthuis, W., Tsujimura, S., Sudholter, E.J.R., van den Berg, A., 2014. Lactate biosensors: current status and outlook. *Anal Bioanal Chem* 406(1), 123-137.

Rathee, K., Dhull, V., Dhull, R., Singh, S., 2016. Biosensors based on electrochemical lactate detection: A comprehensive review. *Biochemistry and biophysics reports* 5, 35-54.

Rawson, T.M., Sharma, S., Georgiou, P., Holmes, A., Cass, A., O'Hare, D., 2017. Towards a minimally invasive device for beta-lactam monitoring in humans. *Electrochemistry Communications* 82, 1-5.

Ren, J., Dean Sherry, A., Malloy, C.R., 2013. Noninvasive monitoring of lactate dynamics in human forearm muscle after exhaustive exercise by 1H-magnetic resonance spectroscopy at 7 tesla. *Magnetic resonance in medicine* 70(3), 610-619.

Rimachi, R., De Carvahlo, F.B., Orellano-Jimenez, C., Cotton, F., Vincent, J., De Backer, D., 2012. Lactate/pyruvate ratio as a marker of tissue hypoxia in circulatory and septic shock. *Anaesthesia and intensive care* 40(3), 427.

Saito, N., Adachi, H., Tanaka, H., Nakata, S., Kawada, N., Oofusa, K., Yoshizato, K., 2017. Interstitial fluid flow-induced growth potential and hyaluronan synthesis of fibroblasts in a fibroblast-populated stretched collagen gel culture. *Biochimica et Biophysica Acta (BBA)-General Subjects* 1861(9), 2261-2273.

Sayeed, M., Murthy, P., 1981. Adenine nucleotide and lactate metabolism in the lung in endotoxin shock. *Circulatory shock* 8(6), 657-666.

Sharma, S., Huang, Z., Rogers, M., Boutelle, M., Cass, A.E., 2016. Evaluation of a minimally invasive glucose biosensor for continuous tissue monitoring. *Anal Bioanal Chem* 408(29), 8427-8435.

Sharma, S., Saeed, A., Johnson, C., Gadegaard, N., Cass, A.E., 2017. Rapid, low cost prototyping of transdermal devices for personal healthcare monitoring. *Sensing and Bio-Sensing Research* 13, 104-108.

Shimomura, T., Sumiya, T., Ono, M., Ito, T., Hanaoka, T.-a., 2012. Amperometric L-lactate biosensor based on screen-printed carbon electrode containing cobalt phthalocyanine, coated with lactate oxidase-mesoporous silica conjugate layer. *Analytica chimica acta* 714, 114-120.

Shinbo, T., Sugiura, M., Kamo, N., 1979. Potentiometric enzyme electrode for lactate. *Analytical Chemistry* 51(1), 100-104.

Stanley, W.C., Gertz, E.W., Wisneski, J.A., Morris, D.L., Neese, R.A., Brooks, G.A., 1985. Systemic lactate kinetics during graded exercise in man. *American Journal of Physiology-Endocrinology And Metabolism* 249(6), E595-E602.

Taurino, I., Sanzò, G., Antiochia, R., Tortolini, C., Mazzei, F., Favero, G., De Micheli, G., Carrara, S., 2016. Recent advances in third generation biosensors based on Au and Pt nanostructured electrodes. *TrAC Trends in Analytical Chemistry* 79, 151-159.

Thomas, N., Lähdesmäki, I., Parviz, B.A., 2012. A contact lens with an integrated lactate sensor. *Sensors and Actuators B: Chemical* 162(1), 128-134.

Umena, Y., Yorita, K., Matsuoka, T., Kita, A., Fukui, K., Morimoto, Y., 2006. The crystal structure of L-lactate oxidase from *Aerococcus viridans* at 2.1 Å resolution reveals the mechanism of strict substrate recognition. *Biochemical and biophysical research communications* 350(2), 249-256.

Valdés-Ramírez, G., Li, Y.-C., Kim, J., Jia, W., Bandodkar, A.J., Nuñez-Flores, R., Miller, P.R., Wu, S.-Y., Narayan, R., Windmiller, J.R., 2014. Microneedle-based self-powered glucose sensor. *Electrochemistry Communications* 47, 58-62.

Valenza, F., Aletti, G., Fossali, T., Chevallard, G., Sacconi, F., Irace, M., Gattinoni, L., 2005. Lactate as a marker of energy failure in critically ill patients: hypothesis. *Critical Care* 9(6), 588.

Ventrelli, L., Marsilio Strambini, L., Barillaro, G., 2015. Microneedles for transdermal biosensing: current picture and future direction. *Advanced healthcare materials* 4(17), 2606-2640.

Windmiller, J.R., Zhou, N., Chuang, M.-C., Valdés-Ramírez, G., Santhosh, P., Miller, P.R., Narayan, R., Wang, J., 2011. Microneedle array-based carbon paste amperometric sensors and biosensors. *Analyst* 136(9), 1846-1851.

Wu, F., Huang, Y., Huang, C., 2005. Chemiluminescence biosensor system for lactic acid using natural animal tissue as recognition element. *Biosensors and Bioelectronics* 21(3), 518-522.

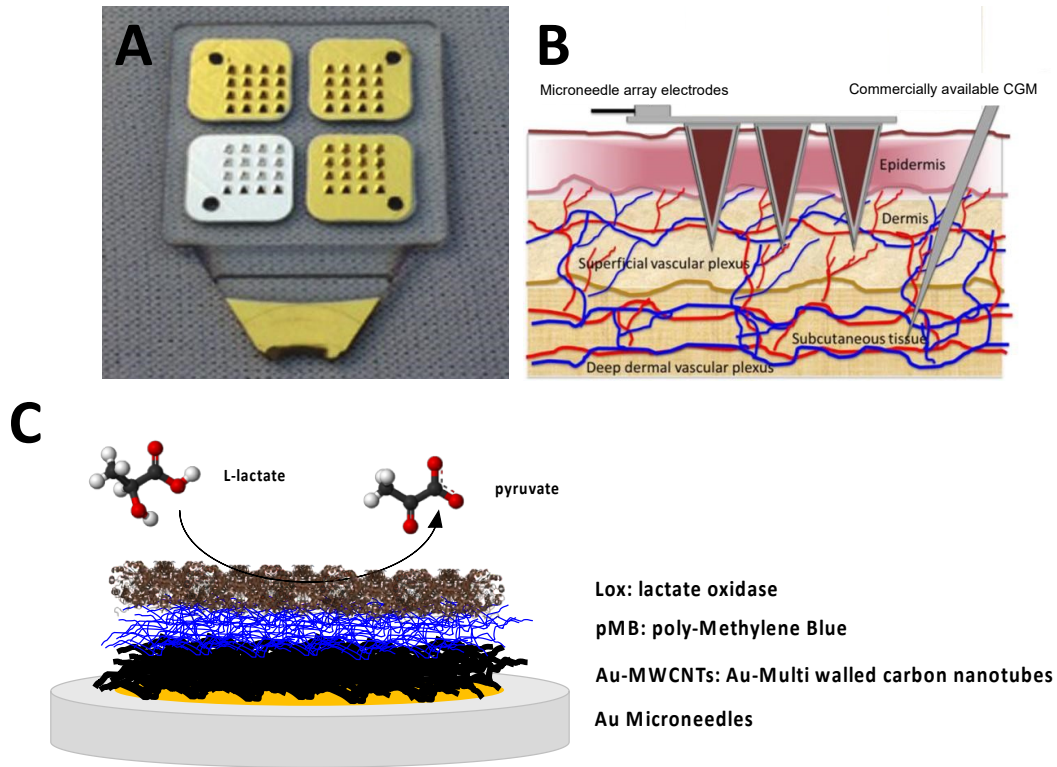


Fig. 1 (A) Polycarbonate structure of four 4x4 microneedle arrays metallized with gold and silver; (B) Sketch of the outermost layers of the human skin, epidermis and dermis and of the two different approaches used (microneedles arrays and commercial CGM devices) to access the interstitial fluid; (C) Schematic representation of the modified electrode. Figures A and B are reproduced from *Sharma et al., 2016* with permission of Springer Berlin Heidelberg.

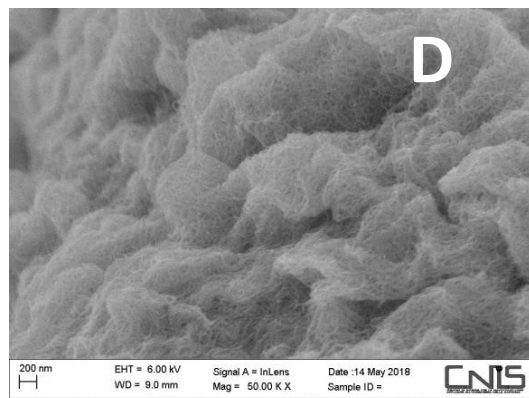
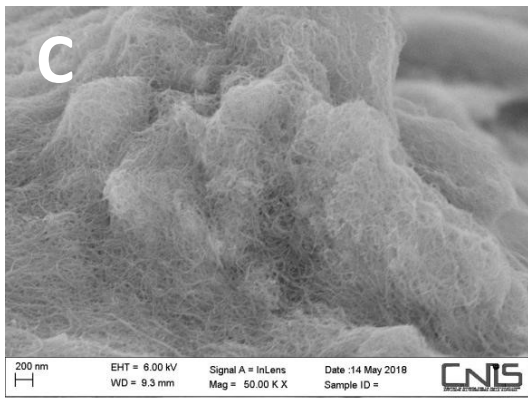
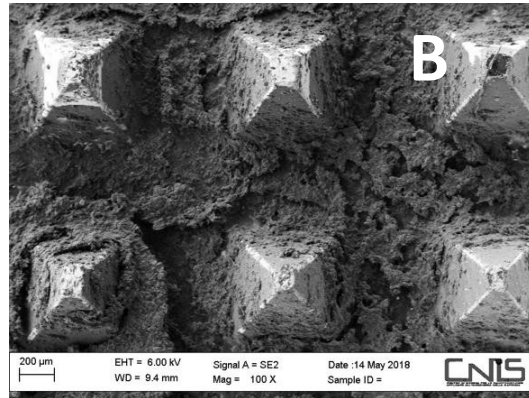
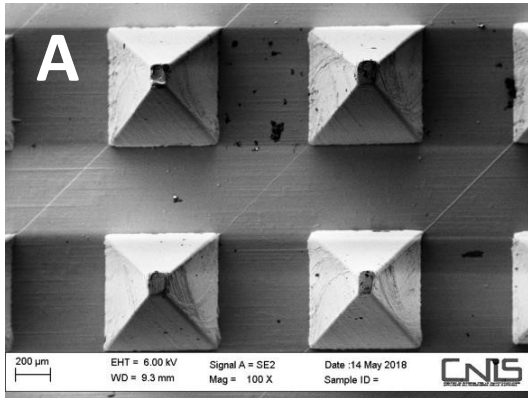


Fig. 2 SEM images of: bare Au microneedle electrode (A); Au microneedle/Au-MWCNTs electrode at two different magnifications (B, C); Au microneedle/Au-MWCNTs/pMB electrode (D).



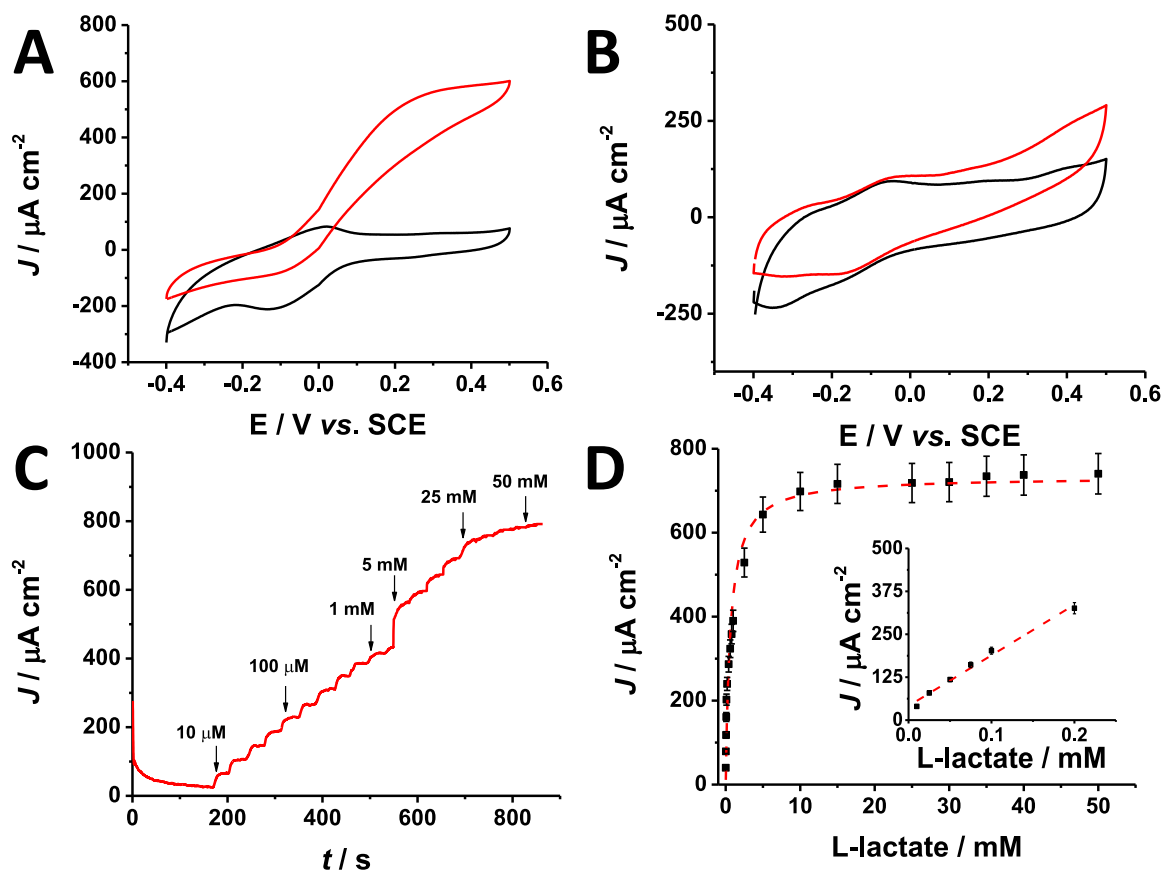


Fig. 3 Cyclic voltammograms of Au microneedle/Au-MWCNTs/pMB/LOX (A) and Au bare/Au-MWCNTs/pMB/LOX in absence (black) and in presence (red) of 10 mM sodium L-lactate in 50 mM PBS buffer pH 7.4 with 137 mM NaCl at  $v = 5 \text{ mV s}^{-1}$ . (C) Chronoamperometric response of Au microneedles/Au-MWCNTs/pMB/LOX in 50 mM PBS buffer with 137 mM NaCl. (D) Calibration curve of the Au microneedles/Au-MWCNTs/pMB/LOX based biosensor in 50 mM PBS buffer with 137 mM NaCl. Inset: low micromolar range. Experimental conditions: applied potential + 0.15 V vs. SCE, adding time = 40 s, under stirring = 400 rpm and  $T = 25 \text{ }^\circ\text{C}$ .

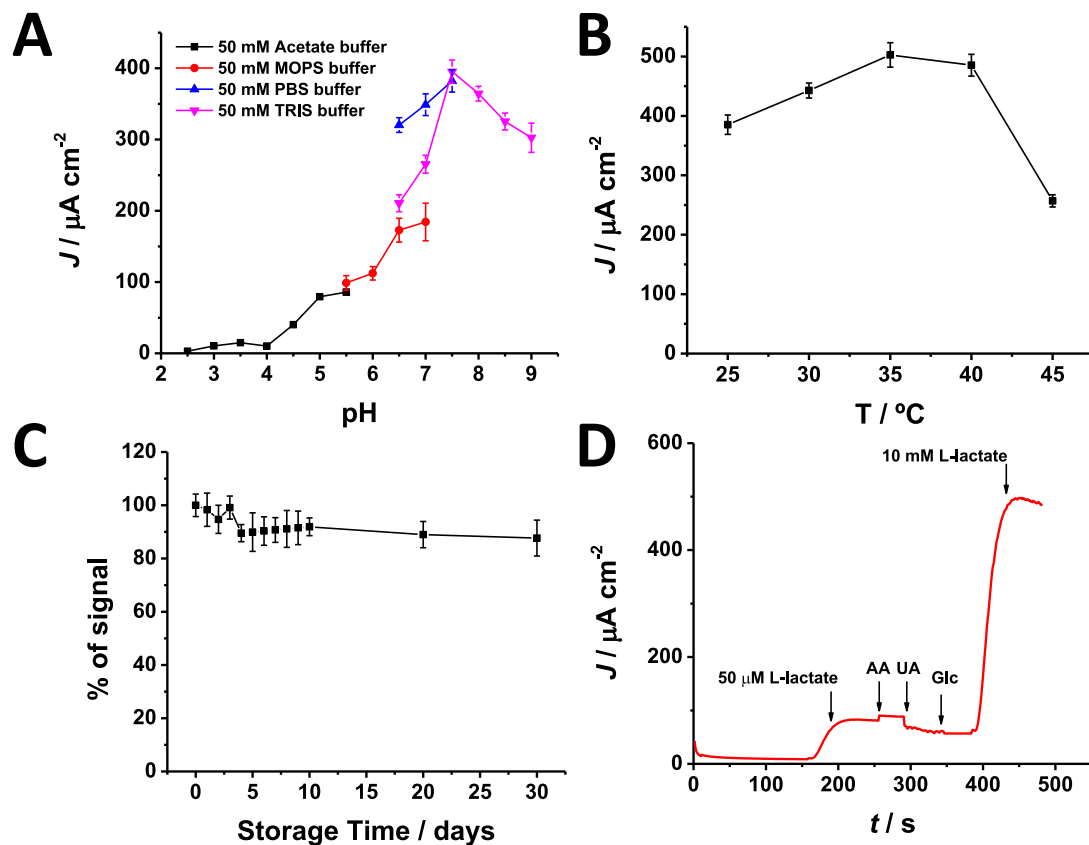


Fig. 4 Effect of different pHs (A) and temperature (B) on Au microneedle/Au-MWCNTs/pMB/LOX based biosensor: 50 mM acetate buffer (black), 50 mM MOPS buffer; 0.2 mM L-lactate (red), 50 mM phosphate buffer (blue) and TRIS buffer (pink). Experimental conditions: 0.2 mM L-lactate, applied potential + 0.15 V. (C) Stability measurements carried out over a period of 30 days in presence of 0.2 mM L-lactate in 50 mM TRIS buffer;  $E_{\text{app}} = 0.150$  vs. SCE;  $T = 25^\circ$ . (D) Influence of interfering compounds on lactate response: 50  $\mu\text{M}$  L-lactate, 50  $\mu\text{M}$  ascorbic acid (AA), 50  $\mu\text{M}$  uric acid (UA), 50  $\mu\text{M}$  glucose (Glc) and 10 mM L-lactate. Experimental conditions: applied potential + 0.15 V vs. SCE, adding time = 40 s, under stirring = 400 rpm and  $T = 25^\circ\text{C}$ .

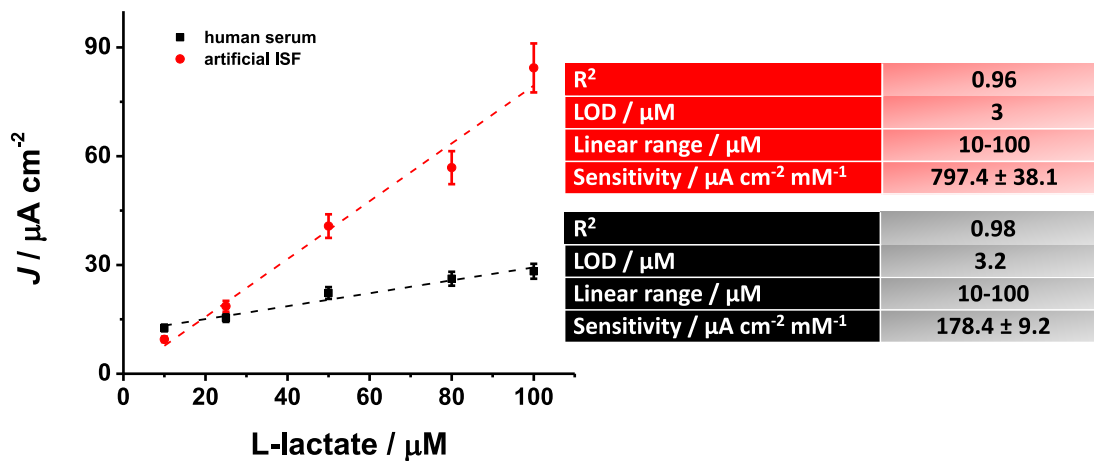


Fig. 5 Calibration curves of the Au microneedles/Au-MWCNTs/pMB/LOX based lactate biosensor in artificial interstitial fluid (red curve) and in human serum (black curve), both spiked with lactate. Experimental conditions: applied potential +0.15 V vs. SCE, adding time = 40 s, under stirring = 400 rpm and T = 25 °C.

Electrode material	Sensing fluid	Sensor type	Linear range (mM)	Sensitivity	Enzyme	Generation	References
AgNPs	sweat	bendable	1-25	$0.26 \mu\text{A mM}^{-1} \text{cm}^{-2}$	<i>Pediococcus sp.</i>	1 <sup>st</sup>	Abrar et al. 2016
CNTs-Ag/AgCl	sweat	bendable	1-20	$10.31 \mu\text{A} \mu\text{M}^{-1} \text{cm}^{-2}$	microorganism	2 <sup>nd</sup>	Wang et al., 2013
Gr + PB, Ag/AgCl integrated in a mouthguard	saliva	printable on curved surface	0.1-1	$0.55 \mu\text{A mM}^{-1}$	microorganism	1 <sup>st</sup>	Wang et al., 2014
Ti/Pd/Pt integrated in contact lens	tears	rigid type film	0-1	$53 \mu\text{A mM}^{-1} \text{cm}^{-2}$	<i>Aerococcus viridans</i>	1 <sup>st</sup>	Thomas et al., 2012
Au microneedles /Au-MWCNTs/pMB	interstitial fluid	bendable	0.01-0.2	$1473.3 \mu\text{A mM}^{-1} \text{cm}^{-2}$	<i>Aerococcus viridans</i>	2 <sup>nd</sup>	this work

Table 1. Comparison with other non invasive amperometric lactate biosensors reported in literature.

**Supplementary Material**

[Click here to download Supplementary Material: Supporting\\_final\\_TC.docx](#)